

INFLUENCE OF A MAGNETIC FIELD ON THE FLOW IN A U-BEND

C. Mistrangelo, L. Bühler*

Karlsruhe Institute of Technology, P.O. Box 3640, 76021 Karlsruhe, Germany

**e-Mail: chiara.mistrangelo@kit.edu*

Liquid metal flow through a circular pipe forming a U-bend is investigated numerically for a constant Reynolds number when a uniform magnetic field is imposed. The influence of the intensity of the applied magnetic field on the flow pattern, pressure and electric current distribution is studied via 3D numerical simulations. It is found that when the magnetic field is weak, a spiral motion develops that is fed mainly by the fluid moving in the boundary regions. By increasing the magnetic field, the stronger electromagnetic forces weaken the vortical flow and significantly affect flow features leading to the formation of an internal field-aligned fluid layer tangent to the inner side of the bend. This layer carries then most of the flow.

Introduction.

Curved pipes are essential components in many technical applications such as heat exchangers, nuclear reactors, industrial piping systems and combustion engines. Hydrodynamic flows in bends are characterized by the occurrence of secondary motion in the form of two counter-rotating vortices known as Dean cells [1]. They are caused by a radial pressure gradient resulting from the centrifugal force acting on the fluid in the curved pipe section. Their presence leads to increased mass and momentum transfer and enhanced cross-sectional mixing. The secondary motion is affected by different parameters such as the curvature ratio and the Reynolds number [2]. Fully developed hydrodynamic flows in curved pipes have been extensively studied both numerically and experimentally [3]. Those analyses consider the characterization of Dean vortices, their stability, developing and turbulent flows [4]. On the other hand, the investigation of the influence of an externally imposed magnetic field on the flow in curved pipes did not receive much attention in the past [5, 6]. In the present paper, we study numerically the magnetohydrodynamic (MHD) flow of a liquid metal in an electrically conducting U-bend with a circular cross-section when a uniform transverse magnetic field is applied in the plane of the bend.

1. Problem definition and mathematical model.

We consider a viscous, incompressible, MHD flow of the liquid metal lead lithium (PbLi) in the geometry shown in Fig. 1a. It features two pipes of circular cross-section connected by a 180° bend, referred to as U-bend. The wall is electrically conducting with

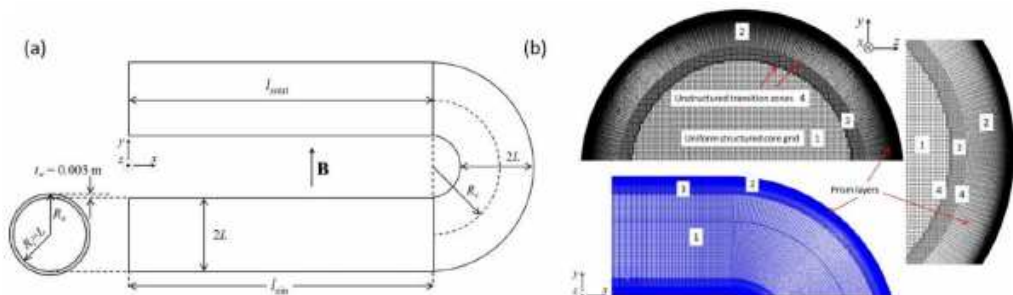


Fig. 1. Geometry used for the study: U-bend of circular cross-section with diameter $2L$ and centreline curvature R_c (a). Details of a hybrid mesh (hexa- and tetrahedral elements) employed for simulations (b).

a thickness $t_w = 3$ mm, and the axial lengths $l_{x\text{in}}$ and $l_{x\text{out}}$ of the inlet and outlet straight pipes were selected depending on flow parameters. The former one is chosen such that the flow in the inlet duct reaches fully developed conditions before entering the bend. The latter one is long enough so that all vortical structures shed in the turning part are damped out before the flow exits the pipe. Fig. 1b shows details of the numerical grid employed for the solution of the problem. The mesh in the pipe cross-section is characterized by a uniform structured core region (1) and wall-parallel prism layers (2) closer to the solid domain. An additional uniform structured zone (3) for the transition between mesh portions 1 and 2 leads to better convergence of the solution. The different structured sub-grids are joined by thin unstructured layers (4).

The investigated liquid metal MHD flow is mathematically described by the momentum equation in which the electromagnetic Lorentz force $\mathbf{j} \times \mathbf{B}$ appears as a source term. The electric current density \mathbf{j} is calculated via Ohm's law and driven by the gradient of the electric potential ϕ and by the induced electric field $\mathbf{v} \times \mathbf{B}$. In the non-dimensional form, the equations read as:

$$\text{N}^{-1}(\partial_t + \mathbf{v} \cdot \nabla)\mathbf{v} = -\nabla p + \text{Ha}^{-2}\nabla^2\mathbf{v} + \mathbf{j} \times \mathbf{B} \quad \text{and} \quad \mathbf{j} = -\nabla\phi + \mathbf{v} \times \mathbf{B}.$$

Conservation of mass $\nabla \cdot \mathbf{v} = 0$ is satisfied by the solution of a pressure equation, and a Poisson equation for the electric potential $\nabla^2\phi = \nabla \cdot (\mathbf{v} \times \mathbf{B})$ ensures the conservation of charge $\nabla \cdot \mathbf{j} = 0$. In the equations above, \mathbf{v} , \mathbf{B} , \mathbf{j} , p and ϕ stand for the velocity, magnetic flux density, current density, pressure and electric potential scaled by the reference quantities u_0 , B_0 , $j_0 = \sigma u_0 B_0$, $p_0 = \sigma u_0 B_0^2 L$ and $\phi_0 = u_0 B_0 L$. The characteristic velocity u_0 is the average velocity in the pipe, B_0 is the magnitude of the applied magnetic field, and $L = R_i = 3.25$ cm is the typical length scale of the problem chosen as the inner radius of the pipe. The flow is characterized by two non-dimensional parameters, the Hartmann number Ha and the interaction parameter N :

$$\text{Ha} = B_0 L \sqrt{\frac{\sigma}{\rho\nu}}, \quad \text{N} = \frac{\sigma L B_0^2}{\rho u_0},$$

where Ha^2 and N denote the ratios of electromagnetic to viscous and inertia forces, respectively. The fluid properties, such as the electric conductivity σ , the kinematic viscosity ν , and the density ρ are taken at a reference temperature of 305°C from [7]. As an alternative control parameter, one could introduce the Reynolds number $\text{Re} = \text{Ha}^2/\text{N}$ that describes the relative importance of inertia and viscous forces. The conductance of the solid wall with conductivity σ_w compared to the conductance of the fluid region is quantified by the wall conductance parameter c (see Fig. 1) [8]:

$$c = \frac{\sigma_w (R_o^2 - R_i^2)}{\sigma (R_o^2 + R_i^2)}.$$

The latter parameter is not required for the mathematical description of the problem as used in the present full numerical simulations since the wall is also resolved by a fine mesh and the electric properties in the wall are determined numerically. However, c is a parameter employed in analytical solutions and, therefore, required for comparison and validation purposes.

As an entrance condition, a fully developed MHD flow is applied with a mean velocity u_0 . At the fluid-wall interface no-slip $\mathbf{v} = 0$ condition is imposed. It is further assumed that no contact resistance is present such that the electric potential and the wall-normal current density are continuous, $\phi = \phi_w$ and $j_n = j_{nw}$.

Influence of a magnetic field on the flow in a U-bend

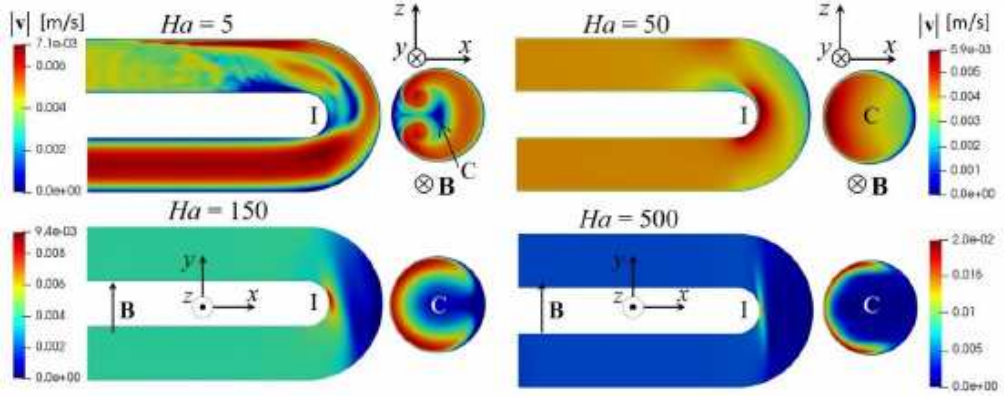


Fig. 2. Velocity magnitude on the symmetry plane $z=0$ and on the (x,z) mid-plane for different Hartmann numbers Ha .

2. Results.

In the following, results are discussed for the flow in a U-bend in the plane of the applied magnetic field $\mathbf{B} = B_0 \hat{y}$, with the curvature ratio $r = L/R_c = 0.5417$, defined as the pipe radius L divided by the radius of the bend curvature R_c , $c = 0.1175$, $Re = 1000$ and different Hartmann numbers Ha .

Fig. 2 shows the velocity magnitude on the symmetry plane at $z=0$ and on the (x,z) middle-plane of the curved pipe for different Hartmann numbers Ha . In the simulations, the outlet pipe is much longer than the one depicted in the figures and has been cut for visualization purposes. At a small Hartmann number $Ha=5$, the flow resembles the hydrodynamic one ($Ha=0$) described in [2] in which, when approaching the bend, the inlet parabolic profile becomes asymmetric and its maximum shifts towards the internal wall of the pipe. Close to the turn, the fluid in the boundary layers starts describing spiral motions when moving upwards along the bend. On the horizontal (x,z) -plane we recognise some typical features of hydrodynamic flow, such as the formation of a secondary flow pattern consisting in Dean-type cells, a separation cell near the inner wall (I) of the bend, and one appearing near the pipe centre (C).

When increasing the strength of the magnetic field (see, e.g., $Ha=50$), the stronger electromagnetic forces tend to stabilize the flow, weakening the spiralling flow structures. As a result, the cell near the internal wall I and the low-velocity zone in the centre C of the U-bend disappear. For more intense magnetic fields, a layer develops tangent to the

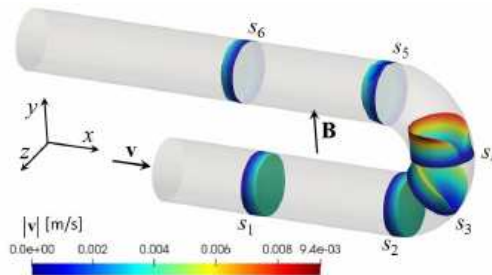


Fig. 3. Flow at $Ha = 150$. Three-dimensional velocity profiles. The coordinate s varies along the pipe centreline.

internal wall of the U-bend, which carries a large portion of the flow rate and becomes more and more aligned with the magnetic field lines with increasing Ha (see $Ha = 500$).

Three-dimensional velocity profiles are plotted in Fig. 3 for the flow at $Ha = 150$ at different positions indicated by the centreline coordinate s of the curved pipe (in Fig. 4a, the polyline along which s varies is marked at the fluid-wall interface by a red dashed line). At $s = s_1$, the MHD flow is laminar and fully developed with a uniform core velocity and slight overspeed in the Roberts boundary layers that form where the magnetic field is parallel and tangent to the pipe wall [9]. At $s = s_2$, close to the bend, the velocity distribution is distorted compared to the fully developed profile with the maximum shifted towards the inner wall of the pipe. At $s = s_3$, on a plane inclined at an angle of 45° with respect to the y -axis, a velocity jet starts developing in the boundary layer along the inner wall of the bend, while near the outer wall there is almost no flow. In the centre of the bend at $s = s_4$, the velocity in the jet increases further. Behind the turn, after passing s_5 , the flow recovers gradually a uniform fully developed profile (see, e.g., $s = s_6$).

In Fig. 4a coloured contours of electric potential are plotted at the fluid-solid interface and on the middle plane of the U-bend for the flow at $Ha = 150$. The variation of the potential along the coordinate s at $z/L = 1$ is shown in Fig. 4b. It can be seen that in a certain portion of the inlet and outlet straight pipes (region 1) the potential is constant

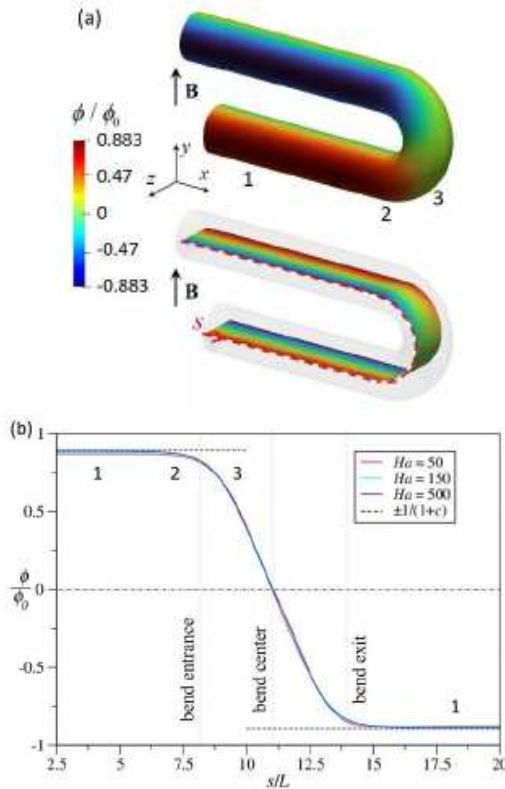


Fig. 4. (a) Contours of the electric potential at the fluid-solid interface and on the middle plane of the U-bend for the flow at $Ha = 150$. (b) Variation of the electric potential along the coordinate s (red dashed line in (a)) at $z/L = 1$ for three Hartmann numbers.

Influence of a magnetic field on the flow in a U-bend

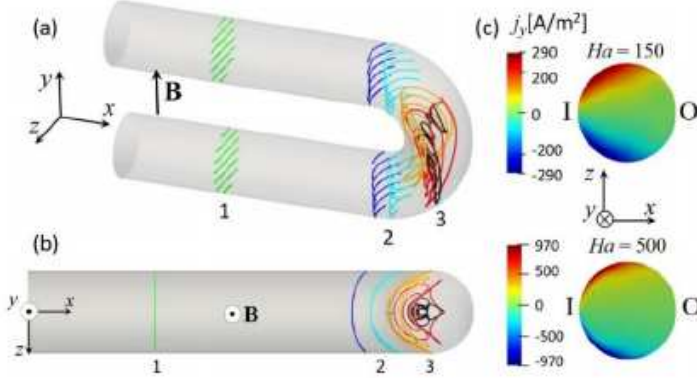


Fig. 5. (a),(b) Electric current paths for the flow at $Ha = 150$ in the fluid domain: upstream and downstream, at a certain distance from the turn, the current closes its path in 2D cross-sectional planes (region 1, green paths). When approaching the bend (zone 2), the axial potential gradient drives additional axial currents (blue, cyan paths). In the bend, complex 3D current loops are present (zone 3). (c) Contours of the y -component of electric current in the (x,z) mid-plane: comparison between flows at $Ha = 150$ and $Ha = 500$.

along the magnetic field lines with variations in the transverse z -direction, as expected in fully developed MHD flows. In this region, near the sides at $z/L = \pm 1$, the normalized electric potential ϕ/ϕ_0 ($z/L = \pm 1$) = ± 0.8903 is in accordance with the estimates for the fully developed pipe flow in electrically conducting pipes at a sufficiently large Ha , where $(\phi/\phi_0)_{\text{FDF}}$ ($z/L = \pm 1$) = $\pm(1 + c)^{-1} = \pm 0.8948$ [8].

In zones (1), where the flow is fully developed, electric currents close through the wall in 2D cross-sectional planes, as seen in Fig. 5 (green streamlines), where typical current paths are illustrated in the fluid domain via both a 3D and a top view of the U-bend. By approaching the turn (zone 2), the electric potential at the side, at $z/L = 1$, decreases along s and it is no longer constant in the magnetic field direction. The resulting electric potential gradient drives additional axial currents so that current loops arch in the streamwise direction (blue and cyan current streamlines). In Fig. 5b, the top (x,z) -view clearly shows the progressive build-up of an axial current component when moving closer to the turn. In the bend (region 3), complex 3D current loops occur which close exclusively in the fluid without entering the wall (orange, black and red paths).

As observed in Fig. 2 for the flow at $Ha = 500$, when the intensity of the magnetic field increases, the main gradients of flow variables are confined in a layer that develops aligned with \mathbf{B} and tangent to the internal wall of the curved pipe. As a result, the currents also tend to flow in this boundary region, as seen in Fig. 5c, where the contours of j_y are depicted on the (x,z) mid-plane of the bend for two Hartmann numbers. This is due to the fact that the pressure in the region of the bend that is separated from the long pipes by the internal layer becomes constant. More details are given when discussing the distribution of the pressure in the entire geometry (see, e.g., Fig. 6).

The interaction of the 3D currents with the imposed magnetic field gives rise to Lorentz forces, which modify locally the pressure distribution.

In Fig. 6 the pressure scaled by p_0 is plotted as a function of the normalized coordinate s/L , both at the centreline ($z/L = 0$) and near the side ($z/L = 1$) for different Hartmann numbers Ha . For strong magnetic fields the red dashed line indicates the

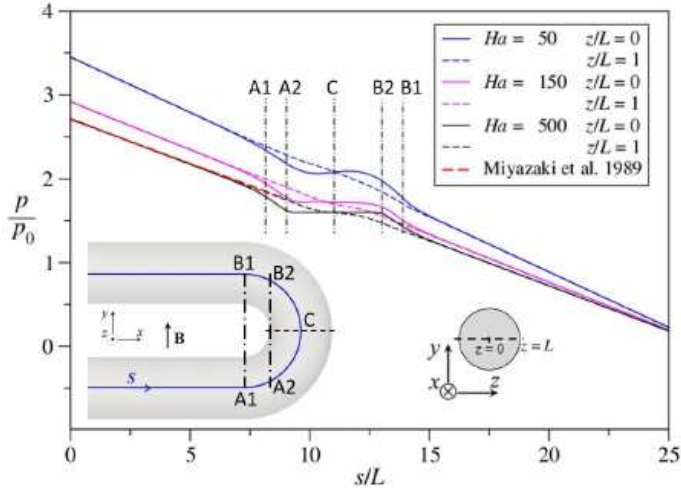


Fig. 6. Distribution of non-dimensional pressure along the central line of the U-bend ($z/L = 0$) and near the side ($z/L = 1$) for flows at different Ha . The dashed red line indicates the pressure variation of the fully developed MHD flow in a pipe B1 according to the formulation of Miyazaki *et al.* [8].

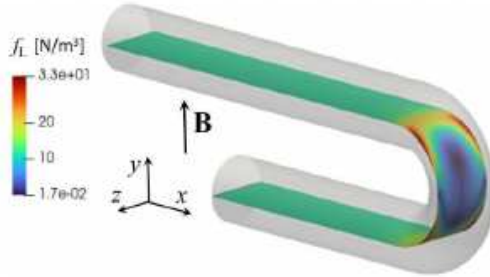


Fig. 7. Magnitude of the electromagnetic force on the middle plane of the U-bend for the flow at $Ha = 150$.

pressure gradient in the fully developed pipe flow according to Miyazaki *et al.* [8], where $\partial p / \partial s = -k_p \sigma u_0 B_0^2$ with $k_p = c / (c + 1)$. When Ha is large enough, the pressure gradient in the straight pipes, at a certain distance from the bend, is in a very good agreement with the one predicted for a fully developed flow.

Close to the bend, the electromagnetic Lorentz forces generated by the 3D currents change the pressure distribution compared to the one in a fully developed pipe flow. When entering the turn (A1), the pressure in the vertical symmetry plane $z/L = 0$ starts decreasing faster than in an analogous fully developed flow. With a sufficiently strong magnetic field, the pressure becomes almost constant between A2 and B2 (see $Ha = 500$). After crossing the internal layer near B2 the pressure gradient approaches gradually the one of the fully developed pipe flow, as in the inlet pipe. Near the sides at $z/L = 1$, more intense transverse Lorentz forces compensate the axial pressure gradients and the 3D MHD effects on pressure are weaker than in the centre of the geometry. The distribution of the magnitude of the electromagnetic Lorentz force is plotted on the middle plane of the geometry in Fig. 7 for the flow at $Ha = 150$.

3. Conclusions.

Numerical simulations have been carried out to study the liquid metal MHD flow in a circular pipe that forms a U-bend in the plane of the applied magnetic field. The influence of the strength of the imposed magnetic field on the velocity and pressure distribution has been investigated for the flow at $Re = 1000$. When the fluid enters the turn, axial currents are induced, which create Lorentz forces that modify essentially the pipe flow compared to fully developed conditions. The secondary flow present at small Ha in the form of Dean-type vortices is suppressed when the magnetic field is increased. At sufficiently large Ha , the flow in the bend is characterized by the formation of a thin fluid layer aligned with \mathbf{B} , tangent to the internal wall of the turn. This layer carries most of the flow.

Acknowledgments.

This work has been carried out in the framework of the EUROfusion Consortium, funded by the European Union via the Euratom Research and Training Programme (Grant Agreement No. 101052200–EUROfusion). Views and opinions expressed are, however, those of the authors only and do not necessarily reflect those of the European Union or the European Commission. Neither the European Union nor the European Commission can be held responsible for them. This work was carried out using super-computer resources, JFRS-1 provided under the EU-JA Broader Approach collaboration in the Computational Simulation Centre of International Fusion Energy Research Centre (IFERC-CSC).

References

- [1] W.R. DEAN. Note on the motion of fluid in a curved pipe. *Philosophical Magazine*, vol. 4 (1927), pp. 208–223.
- [2] R.M.C. SO, H.S. ZHANG AND Y.G. LAI. Secondary cells and separation in developing laminar curved-pipe flows. *Theoret. Comput. Fluid Dynamics*, vol. 3 (1991), pp. 141–162.
- [3] S.A. BERGER, L. TALBOT AND L.S. YAO. Flow in curved pipes. *Annual Review of Fluid Mechanics*, vol. 15 (1983), no. 1, pp. 461–512.
- [4] A. VESTER, R. ÖRLÜ AND P. ALFREDSSON. Turbulent flows in curved pipes: recent advances in experiments, simulations and analysis. *Applied Mechanics Reviews*, vol. 68, 07 2016.
- [5] F. ISSACCI, N.M. GHONIEM AND I. CATTON. Magnetohydrodynamic flow in curved pipe. *Physics of Fluids*, vol. 31 (1988), no. 1, pp. 65–71.
- [6] M. HOQUE AND M. ALAM. Effects of Dean number and curvature on fluid flow through a curved with magnetic field. *Procedia Engineering*, vol. 56 (2013), pp. 245–253.
- [7] D. MARTELLI, A. VENTURINI AND M. UTILI. Literature review of lead-lithium thermophysical properties. *Fusion Engineering and Design*, vol. 138 (2019), pp. 183–195.
- [8] K. MIYAZAKI, S. INOUE AND N. YAMAOKA. MHD pressure drop of liquid metal flow in circular and rectangular ducts under transverse magnetic field. In: *Liquid Metal Magnetohydrodynamics* (J. Lielpeteris and R. Moreau, Eds., Kluwer, 1989), pp. 29–36.

- [9] S. VANTIEGHEM, X. ALBETS-CHICO AND B. KNAEPEN. The velocity profile of laminar MHD flows in circular conducting pipes. *Theoretical and Computational Fluid Dynamics*, vol. 23 (2009), no. 6, pp. 525–533.

Received 24.11.2024